Radiocarbon, Vol 65, Nr 2, 2023, p 357–374 DOI:10.1017/RDC.2023.5

ATMOSPHERIC RADIOCARBON FOR THE PERIOD 1910–2021 RECORDED BY ANNUAL PLANTS

Mariah S Carbone[1,2]* • Tina J Ayers[2] • Christopher H Ebert[1] • Seth M Munson[3] •
Edward A G Schuur[1,2] • Andrew D Richardson[1,4]

[1]Center for Ecosystem Science and Society, Northern Arizona University, Flagstaff, AZ, USA
[2]Department of Biological Sciences, Northern Arizona University, Flagstaff, AZ, USA
[3]Southwest Biological Science Center, U.S. Geological Survey, Flagstaff, AZ, USA
[4]School of Informatics, Computing, and Cyber Systems, Northern Arizona University, Flagstaff, AZ, USA

ABSTRACT. We present a timeseries of $^{14}CO_2$ for the period 1910–2021 recorded by annual plants collected in the southwestern United States, centered near Flagstaff, Arizona. This timeseries is dominated by five commonly occurring annual plant species in the region, which is considered broadly representative of the southern Colorado Plateau. Most samples (1910–2015) were previously archived herbarium specimens, with additional samples harvested from field experiments in 2015–2021. We used this novel timeseries to develop a smoothed local record with uncertainties for "bomb spike" ^{14}C dating of recent terrestrial organic matter. Our results highlight the potential importance of local records, as we document a delayed arrival of the 1963–1964 bomb spike peak, lower values in the 1980s, and elevated values in the last decade in comparison to the most current Northern Hemisphere Zone 2 record. It is impossible to retroactively collect atmospheric samples, but archived annual plants serve as faithful scribes: samples from herbaria around the Earth may be an under-utilized resource to improve understanding of the modern carbon cycle.

KEYWORDS: annual plants, Anthropocene, atmospheric CO_2, bomb spike ^{14}C, carbon cycle, Colorado Plateau, herbarium specimens, RITA, southwestern United States.

INTRODUCTION

Bomb radiocarbon (^{14}C) was produced in the 1950–1960s from atmospheric thermonuclear weapons testing primarily in the Northern Hemisphere (Hesshaimer et al. 1994). This period is increasingly viewed as a near-universal marker of the beginning of the Anthropocene (Turney et al. 2018). Since peaking in the early 1960s, tropospheric $\Delta^{14}C$ has declined over time due to exchange with both the terrestrial (Trumbore 2000) and ocean (Druffel and Suess 1983; Broecker et al. 1985) reservoirs, and also the burning of ^{14}C-free fossil fuels (Hesshaimer and Levin 2000). Fortuitously, bomb ^{14}C provides a unique way to "age" recent (less than ~60 years old) organic matter within 1–3-year resolution by accelerator mass spectrometry (AMS). Thus, quantifying the incorporation of bomb ^{14}C into different pools or tissues allows for estimating residence times and sources of carbon, and is a powerful tracer to study the modern global carbon cycle (Hua and Barbetti 2004).

Tropospheric records of bomb ^{14}C are based on atmospheric CO_2 captured by alkaline solution and flasks from land (e.g., Levin and Kromer 1997; Turnbull et al. 2017), aircraft (e.g., Telegadas 1971), and tree-ring records (e.g., Stuiver and Quay 1981; Yamada et al. 2005) from a small but increasing number of locations on Earth (Hua et al. 2022). These records show differences in the magnitude and timing of the bomb spike across the northern and southern hemispheres due to location and size of bomb detonation, atmospheric transport, and mixing times (Hesshaimer and Levin 2000). With growing interest in studying the global carbon cycle, and increased accessibility of measurements of ^{14}C by AMS, sampling locations added in the past two decades have led to better spatial

---

*Corresponding author. Email: mariah.carbone@nau.edu

and temporal representation (Levin et al. 2022). Hua et al. (2013, 2022) compiled bomb ^{14}C records to develop a set of synthetic datasets that accounted for atmospheric transport and mixing. These calibration curves are specific to five latitudinal zones, and offer improved regional dating accuracy, but the potential for local deviations from these zonal curves has not been fully characterized.

The objective of this work was to develop a century-long bomb ^{14}C record for the southern Colorado Plateau region of the southwestern United States. The Colorado Plateau is a remote area spanning parts of Arizona, Utah, Colorado, and New Mexico. It is characterized by low population density, high elevation, and a generally arid environment. This region has a bimodal precipitation pattern, with winter snow and rain (November–April) and summer monsoon rainfall (July–September). We took advantage of annual plants as unique samplers of atmospheric $^{14}CO_2$ to construct this record. Annual plants can have certain advantages over traditional flask sampling and tree-ring records. First, annual plants complete a lifecycle in less than one year (usually one season). In contrast to long-lived plants like trees, annual plants do not have nonstructural carbon stored from previous years that can be used to grow biomass (e.g., tree rings; Carbone et al. 2013; McDonald et al. 2019) in subsequent years. Thus, with the exception of the initial seed from which it is grown, all carbon in an annual plant is produced from atmospheric CO_2 assimilated within the same year or season. Second, annual plants sample the atmosphere through photosynthesis over many days to months, integrating the atmospheric $^{14}CO_2$ signal over longer periods than flask sampling (minutes to hours). Finally, annual plants are common and widely distributed, and include many crops and non-native weedy species that can be found across ecosystems and therefore are often present in herbaria collections.

The value of annual plants as a proxy for atmospheric $^{14}CO_2$ has been known for many years (Godwin 1969). Annual plants have been used to develop short term (< 10 years) site-specific background atmospheric $^{14}CO_2$ records to accurately date recent terrestrial organic matter when anthropogenic fossil fuel emissions may cause localized lower $^{14}CO_2$ relative to the northern hemispheric average (Carbone et al. 2013; Richardson et al. 2013; Furze et al. 2018, 2020). Creatively, annual plants have been collected across large spatial scales to map and quantify contributions of fossil fuel derived CO_2 to the atmosphere in a given year (Hsueh et al. 2007; Riley et al. 2008; Wang and Pataki 2010, 2012). Most recently, Hüls et al. (2021) created a 75-yr $^{14}CO_2$ record from annual plants (agricultural wheat seed archives) documenting bomb ^{14}C as well as the fossil fuel contributions over the past four decades.

In recent decades, archived herbarium specimens have increasingly been used to study the impact of global change on plants (Meineke et al. 2018; Lang et al. 2019). Specific examples include early studies investigating the effects of rising atmospheric CO_2 on both stomatal density (Woodward 1987) and leaf isotopic composition ($\delta^{13}C$; Peñuelas and AzcónBieto 1992), as well as the effects of increasing temperature on both phenology (Willis et al. 2017) and herbivory (Meineke et al. 2019). We are not aware of herbarium records having been used previously to develop a long-term record of $^{14}CO_2$ in the atmosphere.

Here, we present the application of an herbarium collection of annual plants to develop a smoothed annually resolved record of bomb spike ^{14}C, from 1910 to 2021. We describe the ^{14}C timeseries derived from analysis of 100 individual annual plant samples, and compare these samples to existing western U.S. records, as well as the most current calibration curves for the region. We then use smoothing techniques to develop a synthetic, annual-resolution (summertime values) curve with uncertainty for local dating of terrestrial organic matter. Finally, we discuss the potential to use annual plants, including leveraging of herbaria collections, to complement existing records and further improve understanding of local-to-regional variation in tropospheric $^{14}CO_2$.

METHODS

Annual Plant Samples

Archived annual plant specimens were sampled from the Deaver Herbarium (ASC) at Northern Arizona University in Flagstaff, Arizona, USA (Thiers 2022). We chose herbarium specimens based on annual plants species that had the best representation and abundance during the period 1950–2016. Herbarium specimens in order of abundance include *Xanthisma gracile, Townsendia annua, Plantago argyraea, Erigeron divergens, Bromus rubens*, and *Bromus rigidus*. We prioritized specimens from Coconino and Yavapai counties, which include the southern Colorado Plateau and the adjacent Arizona transition zone of the Mogollon Rim. From each specimen, ~10 mg of leaf, flower, and/or inflorescence material was removed with tweezers, weighed, and placed in a glass vial. We attempted to sample different regions of each specimen, both basal and distal, to ensure that sampling was representative of the atmosphere during the entire period of growth. We were careful to avoid areas of the plant that had been attached with glue or tape to the specimen mounting paper. Figure 1 shows an example of a *Xanthisma gracile* specimen from 1964 that was sampled for ^{14}C.

Additional annual plants were collected by the authors in the Flagstaff area from 2015–2021. These include *Bromus tectorum, Lupinus kingii, Ambrosia acanthicarpa,* and *Solanum lycopersicum.* Plants were harvested at the end of the summer growing season (August and September). After oven-drying at 60°C, leaves were homogenized with mortar and pestle. No chemical pretreatment or washing of plant material was conducted on herbarium specimens or field samples. Potential carbon contamination by dust or human oils was assumed to be minimal in comparison to the carbon in the sample.

^{14}C Analyses

All annual plant samples were prepared for ^{14}C analysis in 2021 at the Arizona Climate and Ecosystem (ACE) Isotope Laboratory at Northern Arizona University. For each sample, approximately 2.5 mg of dry organic matter was weighed into a tin capsule and converted to graphite using the Automated Graphitization Equipment (AGE 3, Ionplus, Switzerland). The ^{14}C content of the graphite was measured using accelerator mass spectrometry (AMS) on a Mini Carbon Dating System (MICADAS, Ionplus, Switzerland). The data (decay corrected $\Delta^{14}C$) are reported in per mil (‰) following standard methods (equation 3.19) summarized in Trumbore et al. (2016). Instrument error is reported for all $\Delta^{14}C$ data; for most samples, it was approximately 1–2‰.

Data Analyses

Annual plant $\Delta^{14}C$ values were compared to the most current synthetic records for the Northern Hemisphere zone 2 from Hua et al. (2022) referred to as NHZ2 summer and NHZ2 monthly from here on. From 1950 to 1972, the NHZ2 summer is a compilation of

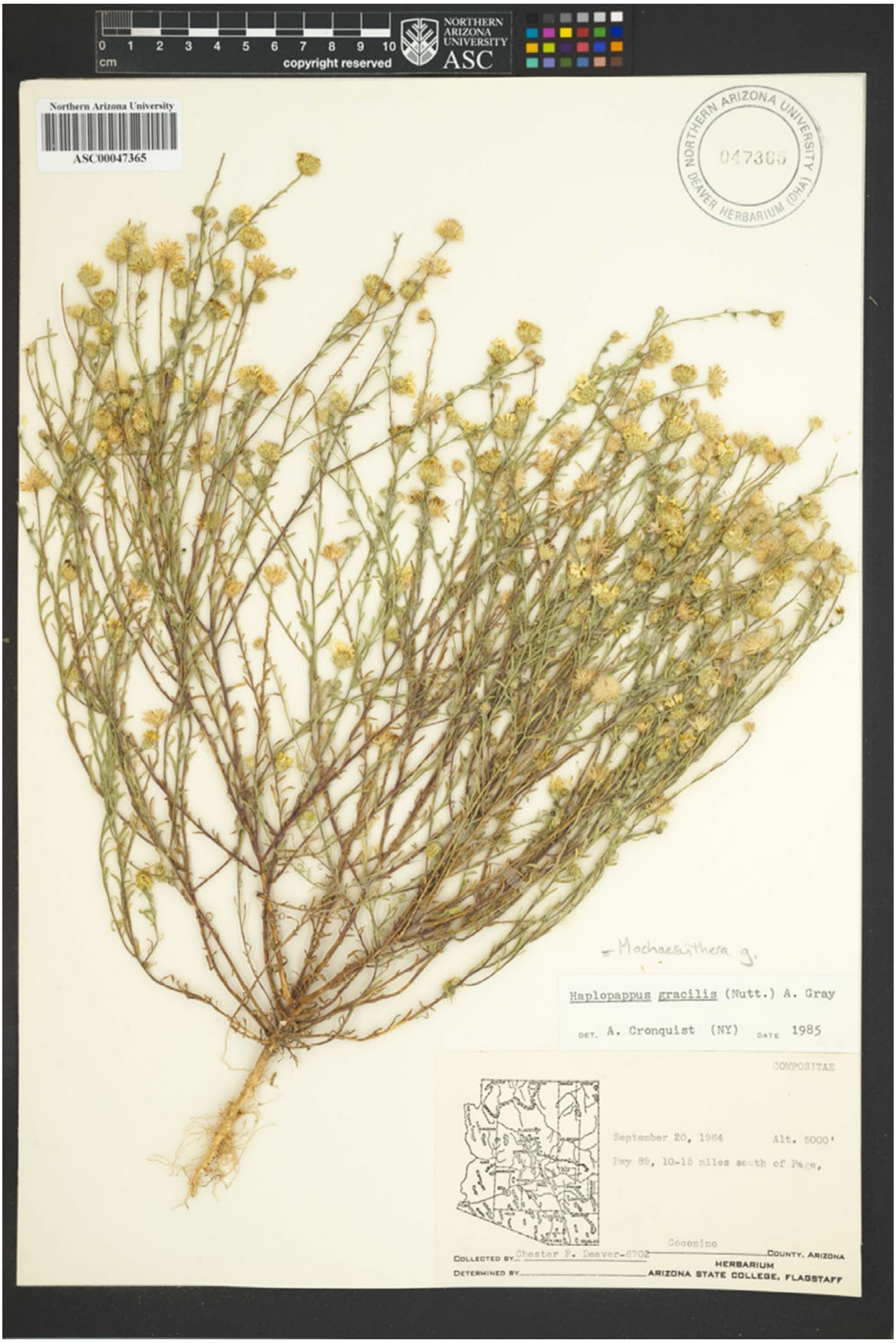

Figure 1 Example of a Deaver Herbarium annual plant specimen (*Xanthisma gracile*) that was harvested in 1964 at the peak of bomb spike in Flagstaff, Arizona, USA.

samples from atmospheric CO_2 captured by alkaline solution (in Spain, Israel, and Senegal) and tree rings (Oregon, Arizona, Mexico, Japan, and South Korea) from clean-air sites. From 1973 to 2019, Hua et al. (2022) does not distinguish different zones for the Northern Hemisphere record and synthesizes many more samples and locations across the Northern Hemisphere. The NHZ2 monthly is derived from similar records as the NHZ2 summer with additional curve fitting and smoothing. We compared our data against the NHZ2 monthly record, with the difference (commonly reported as $\Delta\Delta^{14}C$) calculated as (annual plant $\Delta^{14}C$) – (NHZ2 $\Delta^{14}C$), using the NHZ2 value for the month in which the annual plant was harvested. To account for the potential integration of ^{14}C in annual plant biomass as the plant grows, the difference between annual plant $\Delta^{14}C$ and the mean NHZ2 value of the previous 1, 2, and 5 months was also calculated, representing integration times of 2, 3, and 6 months, respectively. Total error for $\Delta\Delta^{14}C$ was combined in quadrature from the NHZ2 monthly dataset 1σ uncertainty, and the annual plant AMS instrument error.

To develop an annual resolution ^{14}C smoothed record applicable for the southern Colorado Plateau centered near Flagstaff from 1911–2021 (nicknamed RITA, Radiocarbon In Terrestrial Annuals), we used loess smoothing (PROC LOESS in SAS OnDemand for Academics, https://welcome.oda.sas.com/; SAS Institute Inc., Cary NC, USA) to fit a nonparametric local regression surface. We used the original date of collection for all annual plants, and because our dataset was lacking any samples collected between the spring of 1952 and the summer of 1959 we used 1950–1959 data (annual summertime means) from NHZ2 as a secondary constraint. We weighted our observations as the reciprocal of the squared analytical uncertainty (average 2‰), while we weighted NHZ2 summer values using the reported 1σ uncertainty (average 6‰, with a range from 2‰ to 11‰. We then compared the resulting RITA curve (Supplemental Table S1) against the NHZ2 summer curve, as well as the 1850–2015 curve presented by Graven et al. (2017). Uncertainty estimates (1σ) for the RITA curve were calculated from the LOESS regression residuals, and hence these can be interpreted as the expected range within which an individual new measurement might fall, conditional on the data and our regression model.

RESULTS

Annual Plant Sample Characteristics

All 100 annual plant samples (Table 1) grew in Arizona, within proximity to the small city of Flagstaff (Figure 2a). Annual plant samples spanned more than a century, growing between 1910–2021 (Figure 2b), with a larger proportion of samples intentionally selected in the 1960–70s to best capture the rapid changes caused by the bomb spike. Increased sample numbers were also prioritized for the last decade 2010–2021 to better document the flattening of the curve and continuation below 0‰. There were no annual plants sampled in the years 1953–1958. The majority of the annual plant samples were harvested at the end of the spring (May–June) and summer (August–September) seasons in correspondence with the bimodal precipitation pattern in Arizona (Figure 2c). Samples were dominated by those that grew within 50 km of Flagstaff (Figure 2d) at an elevation of over 2000 m (Figure 2e). We estimate the average lifespan, or atmospheric ^{14}C sampling/integration period, of the plants before being harvested was 1–3 months, and at most 6 months.

Annual plant $\Delta^{14}C$ separated by genera are plotted against the NHZ2 summer record (Figure 3a–f). Annual plant $\Delta^{14}C$ ranged from –44‰ in 1951 to 797‰ in 1964. In comparison to the NHZ2 record, no measurable bias in $\Delta^{14}C$ was detected in the

Table 1 Annual plant samples collected near Flagstaff, Arizona, USA. All samples were analyzed for ^{14}C content in 2021 at Northern Arizona University's Arizona Climate and Ecosystems Isotope Laboratory. Plant materials sampled are leaf (L), flower (F) and inflorescence (I, for grasses only indicating the seedhead).

Sample no.	Catalog no.	Family	*Genus species*	Collection date (Y-M-D)	Location (AZ, USA)	Latitude	Longitude	Elevation (m)	Δ^{14}C (‰)	Δ^{14}C error (‰)	Plant material
1	ASC00004979	Asteraceae	*Xanthisma gracile*	1910-08-22	Coconino County	35.1981	−111.6506	2133	−15.3	1.2	L, F
2	ASC00004446	Plantaginaceae	*Plantago argyraea*	1914-08-21	Coconino County	35.1922	−111.6561	2292	−10.0	1.4	L
3	ASC00089981	Asteraceae	*Townsendia annua*	1923-05-14	Yavapai County	34.7210	−111.9297	1060	−24.5	1.6	L
4	ASC00004445	Plantaginaceae	*Plantago argyraea*	1928-07-26	Coconino County	34.9124	−111.7269	2133	−16.0	1.5	L
5	ASC00007838	Asteraceae	*Xanthisma gracile*	1933-09-15	Coconino County	35.1917	−111.6556	2105	−22.7	1.4	L, F
6	ASC00000624	Asteraceae	*Xanthisma gracile*	1936-09-23	Coconino County	35.1981	−111.6506	2100	−31.3	1.5	L, F
7	ASC00002169	Asteraceae	*Xanthisma gracile*	1945-09-18	Coconino County	35.1981	−111.6506	2286	−20.1	1.6	L, F
8	ASC00002782	Asteraceae	*Townsendia annua*	1947-06-23	Yavapai County	34.8697	−111.7603	1314	−33.3	1.5	L
9	ASC00003678	Asteraceae	*Xanthisma gracile*	1950-07-15	Coconino County	35.2114	−111.6125	2103	−31.2	2.0	L, F
10	ASC00005019	Poaceae	*Bromus rubens*	1951-05-12	Yavapai County	34.7675	−111.8928	1219	−44.7	1.2	L, I
11	ASC00007416	Asteraceae	*Townsendia annua*	1952-04-11	Yavapai County	34.7178	−111.9208	1005	−34.0	2.0	L, F
12	ASC00007296	Poaceae	*Bromus rubens*	1952-04-19	Coconino County	36.3078	−112.7611	701	−42.9	1.2	L, I
13	ASC00093853	Plantaginaceae	*Plantago argyraea*	1959-08-19	Coconino County	35.2322	−111.6627	2087	218.0	2.2	L
14	ASC00009525	Asteraceae	*Xanthisma gracile*	1959-08-20	Coconino County	36.0556	−112.1389	2133	222.8	2.3	L, F
15	ASC00012568	Asteraceae	*Erigeron divergens*	1960-07-29	Coconino County	36.7406	−111.4551	2133	195.9	2.0	L
16	ASC00011004	Asteraceae	*Xanthisma gracile*	1960-09-15	Coconino County	35.2492	−112.4212	1524	211.3	2.2	L, F
17	ASC00013297	Poaceae	*Bromus rubens*	1961-04-04	Yavapai County	34.1284	−111.8536	1039	186.8	1.9	L, I
18	ASC00014970	Asteraceae	*Erigeron divergens*	1961-05-13	Coconino County	35.5583	−111.3528	1432	201.5	1.9	L
19	ASC00012435	Asteraceae	*Townsendia annua*	1961-05-18	Coconino County	35.8680	−111.4152	1310	210.8	2.3	L, F
20	ASC00092677	Poaceae	*Bromus richardsonii*	1961-09-10	Greenlee County	33.5520	−109.3032	2740	194.8	1.3	L, I
21	ASC00012927	Poaceae	*Bromus rigidus*	1962-04-28	Coconino County	34.9124	−111.7269	1280	301.6	2.1	L, I
22	ASC00094132	Asteraceae	*Erigeron divergens*	1962-10-26	Coconino County	35.2292	−111.6607	3138	305.1	2.0	L
23	ASC00019364	Asteraceae	*Townsendia annua*	1963-03-31	Yavapai County	34.7372	−112.0002	975	464.2	2.4	L, F
24	ASC00013911	Poaceae	*Bromus tectorum*	1963-05-17	Coconino County	34.8682	−111.7598	1371	309.7	1.5	L, I
25	ASC00013935	Fabaceae	*Lupinus kingii*	1963-07-10	Apache County	34.0712	−109.4663	2468	670.5	1.7	L, F
26	ASC00016250	Asteraceae	*Verbesina encelioides*	1963-12-26	Maricopa County	33.7190	−112.0485	335	773.4	1.8	L, F
27	ASC00016380	Poaceae	*Bromus rubens*	1964-03-19	Yavapai County	34.5483	−112.5007	1615	797.1	2.4	L, I
28	ASC00016382	Poaceae	*Bromus tectorum*	1964-04-21	Coconino County	35.1981	−111.6506	2103	781.1	1.8	L, I
29	ASC00047365	Asteraceae	*Xanthisma gracile*	1964-09-20	Coconino County	36.6911	−111.4728	1524	796.3	2.5	L, F

Table 1 (*Continued*)

Sample no.	Catalog no.	Family	*Genus species*	Collection date (Y-M-D)	Location (AZ, USA)	Latitude	Longitude	Elevation (m)	Δ^{14}C (‰)	Δ^{14}C error (‰)	Plant material
30	ASC00016338	Asteraceae	*Erigeron divergens*	1964-10-10	Yavapai County	34.8697	−111.7603	1219	768.4	2.4	L
31	ASC00015845	Asteraceae	*Townsendia annua*	1965-05-03	Navajo County	34.9022	−110.1575	1508	763.8	2.7	L, F
32	ASC00017302	Poaceae	*Bromus rigidus*	1965-05-19	Coconino County	34.9124	−111.7269	1676	743.8	2.4	L, I
33	ASC00015836	Poaceae	*Bromus rubens*	1965-06-17	Coconino County	34.8819	−111.6756	1828	782.4	2.5	L, I
34	ASC00015814	Asteraceae	*Erigeron divergens*	1965-06-17	Coconino County	34.8819	−111.6756	2133	758.4	2.4	L
35	ASC00040809	Asteraceae	*Erigeron divergens*	1966-04-08	Coconino County	35.1970	−112.2080	2255	688.6	2.3	L
36	ASC00018881	Asteraceae	*Xanthisma gracile*	1967-09-23	Coconino County	34.8697	−111.7249	1310	592.6	2.6	L, F
37	ASC00051501	Asteraceae	*Erigeron divergens*	1968-09-01	Coconino County	34.9068	−111.6529	1314	529.6	2.2	L
38	ASC00051504	Asteraceae	*Erigeron divergens*	1969-05-01	Yavapai County	34.5739	−111.8548	939	595.6	2.3	L
39	ASC00019885	Poaceae	*Bromus rigidus*	1969-05-17	Coconino County	34.9524	−111.7603	1680	538.6	2.2	L, I
40	ASC00019335	Asteraceae	*Xanthisma gracile*	1969-09-11	Yavapai County	34.6207	−111.8268	975	531.8	2.5	L, F
41	ASC00020248	Asteraceae	*Townsendia annua*	1970-04-18	Yavapai County	34.5636	−111.7831	1066	522.2	2.5	L, F
42	ASC00059734	Asteraceae	*Xanthisma gracile*	1971-09-12	Coconino County	36.5850	−111.1103	1676	467.0	2.4	L, F
43	ASC00023713	Asteraceae	*Xanthisma gracile*	1972-07-26	Coconino County	35.1981	−111.6861	2133	461.8	2.6	L, F
44	ASC00059833	Asteraceae	*Townsendia annua*	1973-04-13	Coconino County	36.0209	−111.4122	1219	443.7	2.4	L, F
45	ASC00024918	Plantaginaceae	*Plantago argyraea*	1973-09-03	Coconino County	35.0949	−111.7013	2073	426.2	2.5	L
46	ASC00042928	Asteraceae	*Xanthisma gracile*	1975-08-27	Coconino County	35.1592	−111.7317	2133	371.9	2.4	L, F
47	ASC00030213	Asteraceae	*Xanthisma gracile*	1976-09-04	Coconino County	35.2114	−111.6125	2103	346.3	2.3	L, F
48	ASC00030757	Asteraceae	*Townsendia annua*	1977-04-17	Yavapai County	34.7372	−112.0002	1059	333.7	2.2	L, F
49	ASC00051759	Plantaginaceae	*Plantago argyraea*	1978-09-26	Coconino County	34.8682	−111.4982	2225	317.5	1.3	L
50	ASC00060476	Asteraceae	*Townsendia annua*	1979-05-12	Yavapai County	34.7537	−111.9124	1066	291.4	1.3	L, F
51	ASC00033874	Asteraceae	*Xanthisma gracile*	1979-09-15	Coconino County	35.4077	−111.8510	2438	295.1	1.3	L, F
52	ASC00057181	Asteraceae	*Erigeron divergens*	1980-10-04	Coconino County	35.2593	−111.6928	2267	279.4	2.0	L
53	ASC00037767	Asteraceae	*Erigeron divergens*	1982-09-09	Coconino County	35.2447	−111.5867	2142	229.0	2.1	L
54	ASC00038369	Asteraceae	*Townsendia annua*	1983-04-16	Yavapai County	34.5123	−111.7913	975	227.0	1.3	L, F
55	ASC00039676	Asteraceae	*Xanthisma gracile*	1983-09-09	Coconino County	35.1981	−111.6506	2133	229.9	1.3	L, F
56	ASC00039871	Poaceae	*Bromus rubens.*	1984-03-26	Yavapai County	34.2323	−112.1563	865	213.9	2.0	L, I
57	ASC00044328	Asteraceae	*Xanthisma gracile*	1985-07-14	Coconino County	35.2301	−111.6044	2164	195.1	1.3	L, F
58	ASC00050637	Plantaginaceae	*Plantago argyraea*	1985-08-02	Coconino County	35.2326	−111.6218	2164	203.5	2.1	L
59	ASC00044488	Asteraceae	*Erigeron divergens*	1986-03-16	Coconino County	36.2429	−111.7365	1036	179.6	2.0	L
60	ASC00058249	Plantaginaceae	*Plantago argyraea*	1987-08-13	Coconino County	34.4849	−111.2229	2133	166.8	2.1	L

(*Continued*)

Table 1 (*Continued*)

Sample no.	Catalog no.	Family	*Genus species*	Collection date (Y-M-D)	Location (AZ, USA)	Latitude	Longitude	Elevation (m)	$\Delta^{14}C$ (‰)	$\Delta^{14}C$ error (‰)	Plant material
61	ASC00068047	Asteraceae	*Erigeron divergens*	1988-04-27	Yavapai County	34.6483	−111.7536	1097	156.6	1.3	L
62	ASC00074116	Asteraceae	*Xanthisma gracile*	1989-09-13	Coconino County	35.3587	−111.6197	2606	160.4	2.1	L, F
63	ASC00058142	Asteraceae	*Townsendia annua*	1991-05-01	Yavapai County	34.6167	−111.8333	1097	127.2	2.0	L, F
64	ASC00054919	Asteraceae	*Xanthisma gracile*	1992-08-14	Yavapai County	34.9649	−112.1020	1706	129.8	2.1	L, F
65	ASC00057960	Asteraceae	*Xanthisma gracile*	1994-09-12	Coconino County	35.1981	−111.6506	2072	114.9	2.3	L, F
66	ASC00058233	Asteraceae	*Townsendia annua*	1995-04-28	Yavapai County	34.6489	−111.7572	1081	108.4	1.2	L, F
67	ASC00059256	Plantaginaceae	*Plantago argyraea*	1995-07-17	Coconino County	35.1981	−111.6506	2134	112.8	1.2	L
68	ASC00094729	Asteraceae	*Erigeron divergens*	1996-05-04	Yavapai County	34.7696	−112.0407	1010	92.7	1.3	L
69	ASC00119880	Asteraceae	*Xanthisma gracile*	1997-09-29	Coconino County	35.1667	−111.5333	2057	96.3	1.2	L, F
70	ASC00065597	Asteraceae	*Xanthisma gracile*	1998-09-24	Yavapai County	34.9225	−112.8425	1580	95.8	1.2	L, F
71	ASC00069668	Asteraceae	*Xanthisma gracile*	2001-09-02	Coconino County	35.1417	−111.6750	2134	78.7	1.2	L, F
72	ASC00083560	Asteraceae	*Xanthisma gracile*	2002-05-04	Yavapai County	34.9207	−111.9100	1430	56.3	1.2	L, F
73	ASC00076203	Asteraceae	*Townsendia annua*	2003-01-26	Yavapai County	34.7972	−111.7567	1295	70.6	1.2	L, F
74	ASC00077184	Plantaginaceae	*Plantago argyraea*	2003-09-06	Coconino County	35.0556	−111.8431	2048	73.3	1.3	L
75	ASC00078338	Asteraceae	*Townsendia annua*	2004-06-18	Yavapai County	34.8122	−111.8247	1182	68.3	1.2	L, F
76	ASC00085059	Plantaginaceae	*Plantago argyraea*	2005-06-29	Coconino County	35.5932	−111.8031	1960	56.5	1.2	L, F
77	ASC00080765	Plantaginaceae	*Plantago argyraea*	2005-08-30	Coconino County	34.5663	−111.3314	2087	58.6	1.2	L
78	ASC00096924	Plantaginaceae	*Plantago argyraea*	2006-08-24	Coconino County	35.1636	−112.1601	2143	54.8	1.2	L
79	ASC00092591	Asteraceae	*Xanthisma gracile*	2008-04-29	Coconino County	36.3969	−112.5144	870	40.5	1.3	L
80	ASC00092694	Asteraceae	*Xanthisma gracile*	2009-08-16	Coconino County	35.6770	−112.4042	1680	43.6	1.2	L, F
81	ASC00104633	Asteraceae	*Erigeron divergens*	2010-08-04	Coconino County	36.5404	−112.3416	2300	35.0	1.3	L
82	ASC00116769	Asteraceae	*Xanthisma gracile*	2011-09-16	Yavapai County	34.5407	−111.8263	950	33.3	1.3	L, F
83	ASC00103054	Plantaginaceae	*Plantago argyraea*	2012-09-30	Coconino County	35.3821	−111.5823	2225	32.3	1.5	L
84	ASC00111281	Asteraceae	*Townsendia annua*	2013-05-05	Coconino County	36.1243	−111.5798	1423	23.2	1.2	L, F
85	ASC00112538	Plantaginaceae	*Plantago argyraea*	2013-09-07	Coconino County	34.5130	−111.3623	2065	12.7	1.2	L
86	ASC00107499	Asteraceae	*Erigeron divergens*	2014-06-07	Coconino County	35.6950	−112.5124	1676	18.6	1.2	L
87	ASC00112117	Asteraceae	*Townsendia annua*	2015-04-06	Yavapai County	34.7557	−111.9995	1006	14.5	1.1	L, F
88	NA	Fabaceae	*Lupinus kingii*	2015-08-01	Coconino County	35.1603	−111.7306	2169	19.9	1.2	L
89	NA	Fabaceae	*Lupinus kingii*	2016-08-01	Coconino County	35.1603	−111.7306	2169	16.2	1.2	L
90	NA	Fabaceae	*Lupinus kingii*	2017-08-01	Coconino County	35.1603	−111.7306	2169	11.7	1.2	L
91	NA	Fabaceae	*Lupinus kingii*	2018-08-01	Coconino County	35.1603	−111.7306	2169	6.0	1.2	L
92	NA	Fabaceae	*Lupinus kingii*	2019-08-01	Coconino County	35.1603	−111.7306	2169	6.8	1.2	L

Table 1 (*Continued*)

Sample no.	Catalog no.	Family	*Genus species*	Collection date (Y-M-D)	Location (AZ, USA)	Latitude	Longitude	Elevation (m)	$\Delta^{14}C$ (‰)	$\Delta^{14}C$ error (‰)	Plant material
93	NA	Asteraceae	*Ambrosia acanthicarpa*	2019-09-15	Coconino County	35.1796	−111.6050	2091	3.8	1.2	L
94	NA	Solanaceae	*Solanum lycopersicum*	2019-09-15	Coconino County	35.1796	−111.6050	2091	2.8	1.2	L
95	NA	Poaceae	*Bromus tectorum*	2019-09-15	Coconino County	35.1796	−111.6050	2091	4.2	1.2	L, I
96	NA	Asteraceae	*Ambrosia acanthicarpa*	2020-09-15	Coconino County	35.1796	−111.6050	2091	1.4	1.2	L
97	NA	Solanaceae	*Solanum lycopersicum*	2020-09-15	Coconino County	35.1796	−111.6050	2091	1.1	1.2	L
98	NA	Poaceae	*Bromus tectorum*	2020-09-15	Coconino County	35.1796	−111.6050	2091	0.8	1.2	L, I
99	NA	Asteraceae	*Ambrosia acanthicarpa*	2021-09-18	Coconino County	35.1796	−111.6050	2091	0.4	1.8	L
100	NA	Poaceae	*Bromus tectorum*	2021-09-18	Coconino County	35.1796	−111.6050	2091	0.8	1.9	L, I

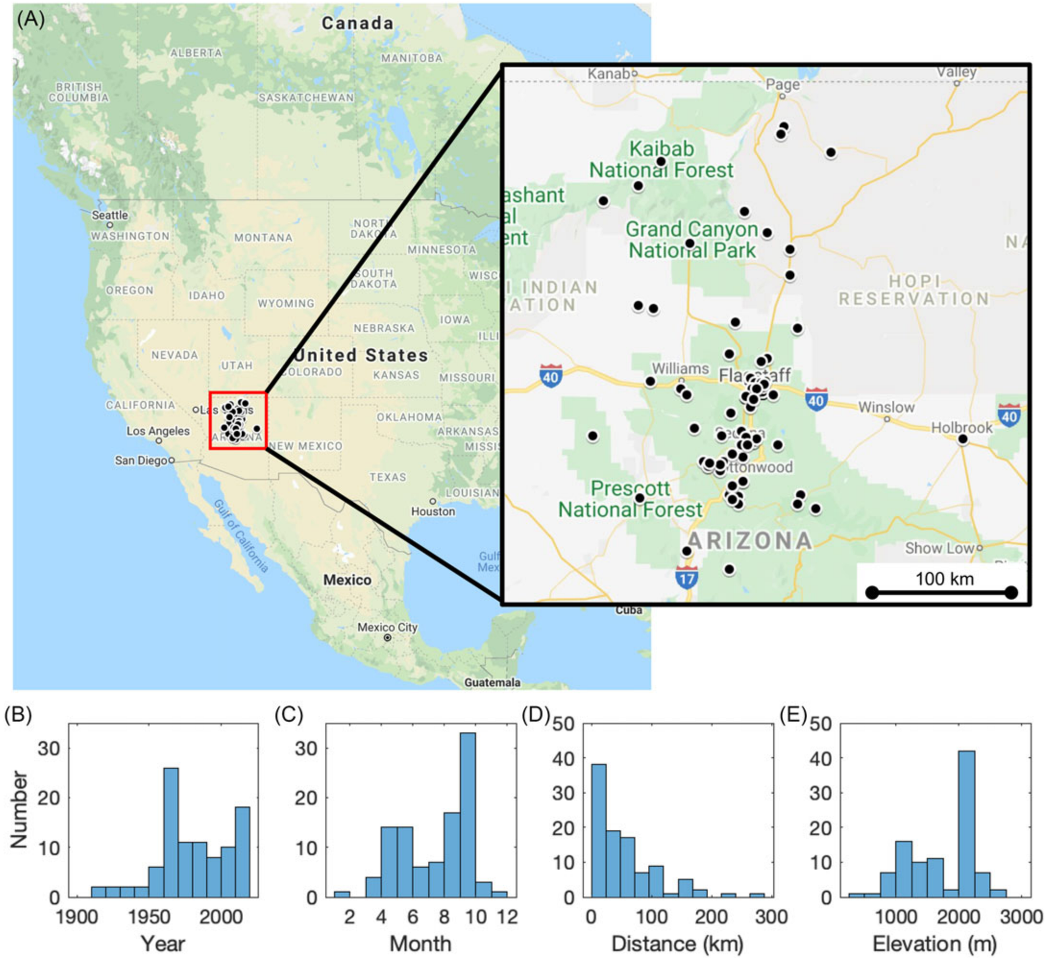

Figure 2 Annual plant sample characteristics. (A) map showing North America with inset of the area surrounding Flagstaff; black dots represent locations where the 100 annual plant samples were collected. Histograms of annual plant samples (B) year of growth; (C) month of sample collection; (D) distance (km) from Flagstaff, AZ, USA; and (E) elevation (m).

samples when $\Delta\Delta^{14}C$ was analyzed by genera of annual plant, elevation, or proximity to Flagstaff. There was a minor bias in $\Delta^{14}C$ depending on month of harvest (see Supplemental Figures S1 and S2a–c). The samples that deviate largely from the NHZ2 record ($\Delta\Delta^{14}C < -100‰$) in Supplemental Figures S1 and S2 occurred between October 1962 and July of 1963 and are discussed below.

Pre-Bomb ^{14}C

The pre-bomb period with samples between 1910 and 1952 shows a strong decline with a slope of –0.6‰ per year ($r^2 = 0.7$ $p<0.001$; Figure 3b). This trend is similar to that observed previously (Stuiver and Quay 1981). The decline in the $\Delta^{14}CO_2$ of the atmosphere is called

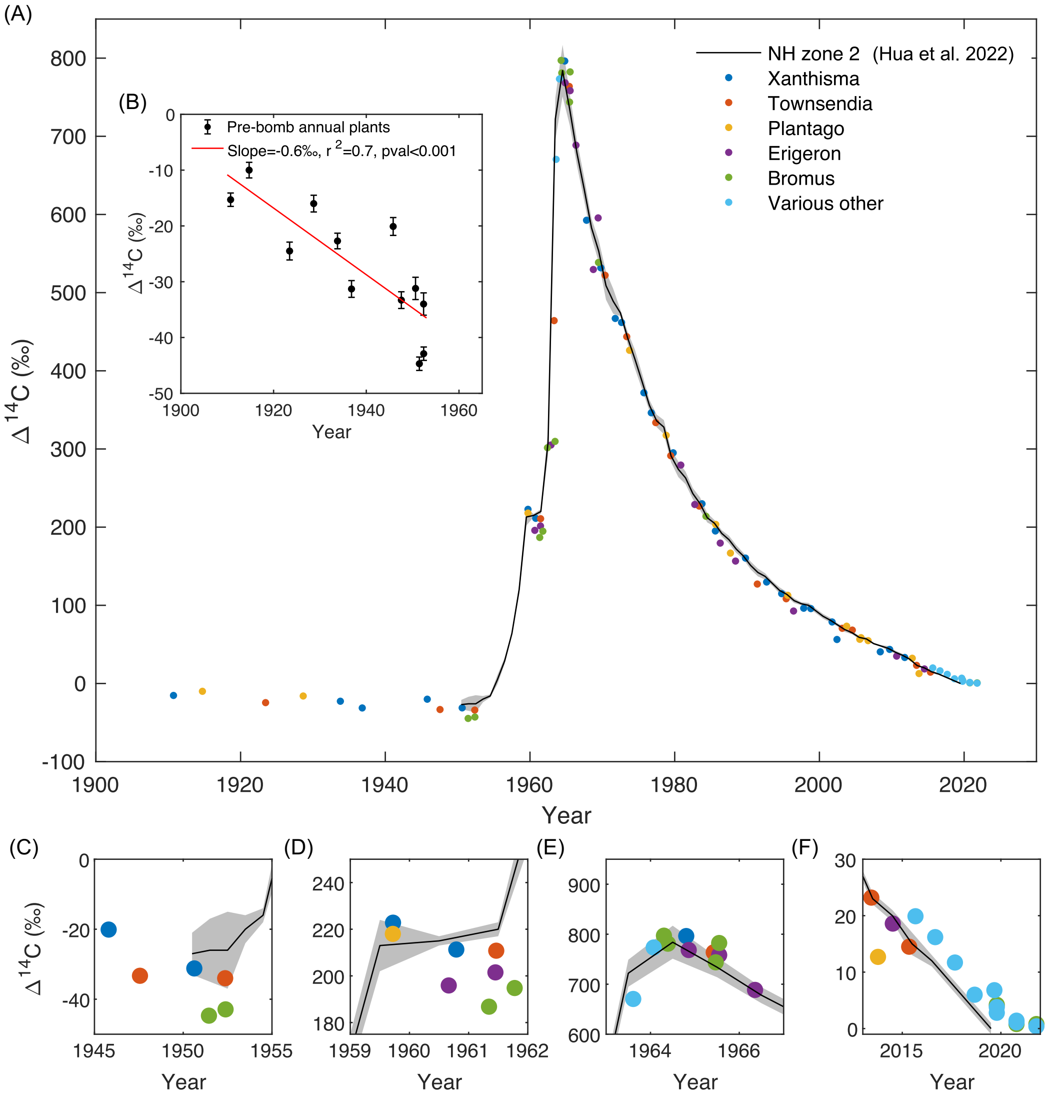

Figure 3 Radiocarbon data (‰). (A) For 100 annual plant samples with *Xanthisma* (blue), *Townsendia* (red), *Plantago* (orange), *Erigeron* (purple), *Bromus* (green), Various other species (light blue). Error is smaller than the size of the symbol. Black line is the summertime annual zone 2 Northern Hemispheric record from Hua et al. (2022) with reported error shaded grey. (B) Linear regression of pre-bomb period (1910–1952; ‰ ± instrument error). (C–F) Zoomed-in plots of same data shown in (A) for specific years; y-axis plots differ across plots. Error is much smaller than the size of the symbol.

the Suess effect (Keeling 1979) following work by Hans Suess (Suess 1955; Revelle and Suess 1957) and is caused by the addition of ^{14}C-free CO_2 to the atmosphere from anthropogenic burning of fossil fuels. However, the annual plant sample $\Delta^{14}C$ values are lower (–8±2‰, mean ± 1SE, n = 11) than the NHZ2 record, indicating a higher local anthropogenic background which coincides with major timber and railroad industries centered in Flagstaff (Reid 2014).

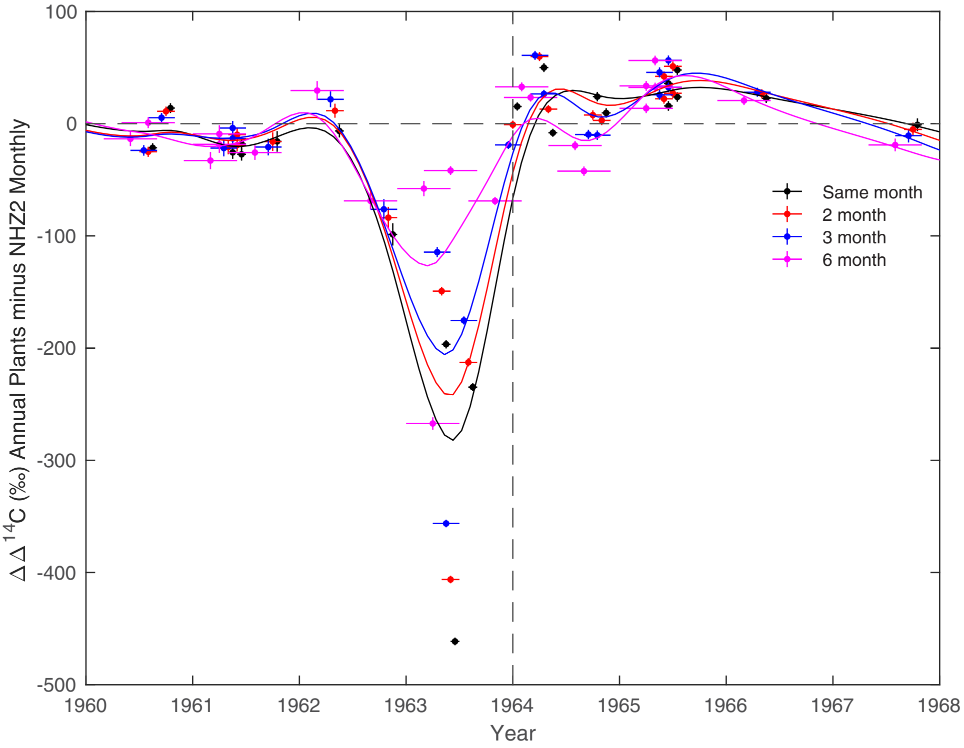

Figure 4 Difference ($\Delta\Delta^{14}C$‰) between the annual plant radiocarbon data and NH zone 2 monthly radiocarbon record from Hua et al. (2022) for integration times of the same month (black dots), 2 months (red dots), 3 months (blue dots), and 6 months (magenta dots). Smoothed spline lines of same colors to show patterns more clearly. X error bars represent the integration time of the NH zone 2 record. Y error bars represent ± combined reported error of both datasets. Dashed horizontal line is 0‰. Dashed vertical line is January 1964.

Bomb Spike ^{14}C

Differences between the NHZ2 record and the annual plants occurs with the rise and peak of the bomb spike in the 1960s. Figure 4 shows the difference in $\Delta^{14}C$ between the annual plant samples and the NHZ2 monthly record where values below zero pre-1964 indicate the annual plant values were lower than the NHZ2 monthly record and values above zero post-1964 indicate annual plant values were higher than the record. This suggests a delayed rise (1962–1963) and fall (1964–1966) in atmospheric $\Delta^{14}C$ in comparison to the NHZ2 monthly record. We explored whether some of this difference in timing could be due to different integration time (or growing time) of the plants. Increasing the integration time improved the agreement of the records, however even with a 6-month integration time (maximum estimated for these plant species, and likely not most representative) there is still a delay in peak of the bomb spike in comparison to the NHZ2 records.

The annual plants have elevated $\Delta^{14}C$ in comparison to the NHZ2 records since 2015, differing from the summer values by as much as 4‰ (3±1‰, mean ± 1SE, n = 8), and only reaching zero in 2021, one to two years later than NHZ2 (Figure 3f). Finally, there is a noticeable flattening of the curve in 2020 and 2021, attributed to reduced fossil fuel emissions during the COVID-19 pandemic (Liu et al. 2020).

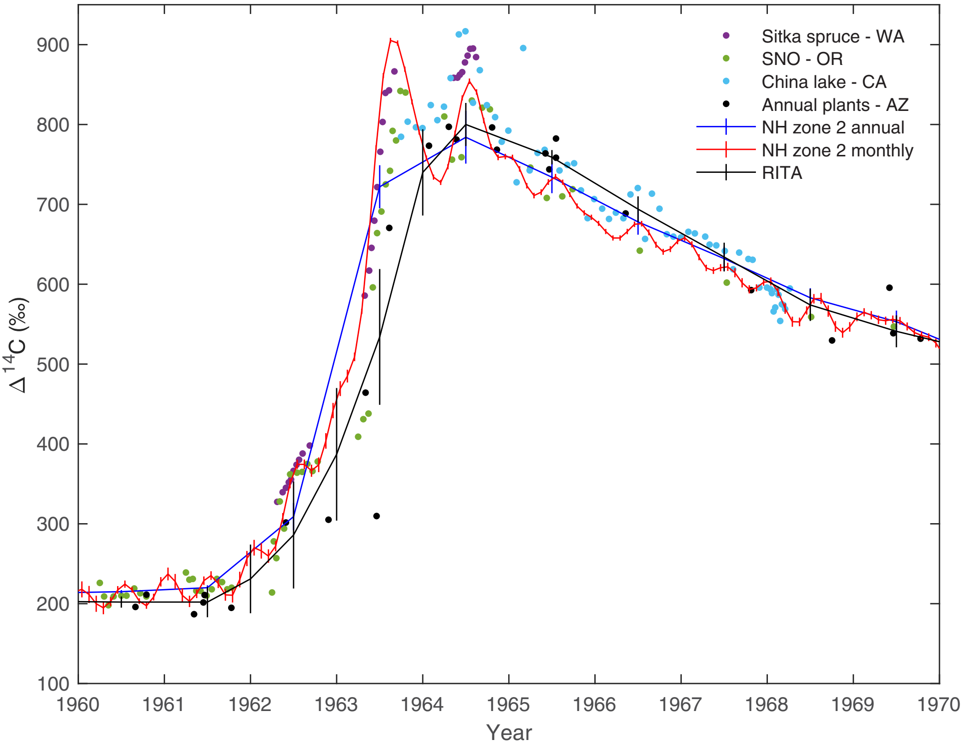

Figure 5 Comparison of $\Delta^{14}C$‰ of subannual tree ring records from Washington (Sitka spruce, blue dots), Oregon (SNO White oak, red dots), atmospheric records from California (China lake, light blue dots), annual plant radiocarbon data (black dots), RITA record (black line), NH zone 2 annual (blue line) and NH zone 2 monthly (red line) radiocarbon record from Hua et al. (2022). Y error bars represent reported uncertainty estimates.

RITA Curve

Discrepancies between our annual plant samples and the most current synthetic record (see Figures 4 and 5) justify the need for more local records for accurate ^{14}C dating of terrestrial organic matter. While generally similar to annual-resolution summer atmospheric $\Delta^{14}C$ records presented by Hua (NHZ2) and Graven et al. (2017), our smoothed RITA curve (Supplemental Table S1) is slightly but consistently lower (more negative $\Delta^{14}C$, by ≈6±2‰, mean ± 1SD) than the Graven curve over the period 1910–1949; the average RITA uncertainty over this period is 5‰. RITA does not rise as rapidly in the early 1960s as either NHZ2 or Graven, although RITA's peak value (800 ± 27‰, mean ± 1σ) in the summer of 1964 is intermediate between NHZ2 (784 ± 33‰) and Graven (836‰). In individual years between 1970 and 1985, deviations of up to ±15‰ between RITA and both NHZ2 and Graven are common. The RITA uncertainty during this period is 7‰ vs. NHZ2 of 9‰. Beginning in 1988, when RITA (at 158±6‰) is lower than either NHZ2 (172 ± 5‰) or Graven (175‰), the distance between all three curves progressively shrinks over the following two and a half decades. By about 2000, the difference between the three curves is reliably less than 5‰, which is comparable to the year-over-year decrease in $\Delta^{14}C$ in all three curves, and similar in magnitude to the RITA uncertainty of 6‰. Intriguingly, since the summer of 2015 RITA has been somewhat higher than NHZ2, particularly in the most recent years. The strong 1-year lag autocorrelation ($r = 0.84$, over the period 1980–2019) of differences between RITA and NHZ2 shows that there are systematic discrepancies between our local record and NHZ2, which persist over time and cannot be attributed to random error.

NH Zone 2

In Figure 5, we compare the annual plant data and RITA record to the NHZ2 curves (annual and monthly), and existing bomb ^{14}C records of subannual tree rings of Sitka spruce from Washington (Grootes et al. 1989), the Sheridan Novitiate Oak (SNO; white oak) in Oregon (Cain et al. 2018), and atmospheric CO_2 captured by NaOH at China Lake, California (Berger et al. 1965, 1966, 1967, 1968, 1969, 1987). The datasets are difficult to quantitatively compare due to differences in the timing of sample collections, but visually the annual plant record and RITA curve have a delayed rise and also a muted bomb peak in comparison to the other records. The annual plant data and RITA record are most similar to the NHZ2 curve, confirming the location of the Flagstaff region within NH Zone 2 along with the Oregon record, whereas the Washington and California records are believed to be in NH Zone 1 (Hua et al. 2022).

DISCUSSION

Unique Regional ^{14}C Record

Our annual plant record of $^{14}CO_2$, derived primarily from herbarium specimens, generally agrees with the regional synthetic record by Hua et al. (2022), but, surprisingly, our data show that there is some evidence for a more delayed arrival of the bomb spike in the southwestern U.S. than has been previously believed. With annual plants, we were able to identify independent herbarium specimens that differed in their active growing season, and spring versus summer phenologies, due to the steep elevation and climate gradient in Arizona. This sampling allowed for fine resolution independent ^{14}C measurements in October of 1962, March, May, and July of 1963 that recorded a delayed arrival of the rise in the bomb spike. Additional specimens in 1964–66 recorded a delay in the subsequent decline in the bomb spike. By broadening our search parameters to include a wider radius around Flagstaff, it may be possible to include samples from a larger number of sites, all of which could still be considered "regional," and thereby improve the temporal resolution of our record during this period when the atmospheric $^{14}CO_2$ signal is extremely dynamic. This delay is most likely due to atmospheric circulation, where the polar and sub-tropical jet moved northward during this time period introducing air masses from the south with lower $\Delta^{14}CO_2$ values (Hua et al. 2022). Another explanation for the delay could be that the annual plants are not sampling the well-mixed atmosphere due to their proximity to the soil surface and are thus influenced by microbial decomposition and plant respiration sources, which would not yet have incorporated bomb carbon at this time. But, in the region we sampled, the vegetation canopy tends to be very open, and the near-surface air space is extremely well ventilated. Finally, we also note that Flagstaff falls ~600–650 km between multiple testing sites in Nevada (upwind) and New Mexico (downwind), where low-yield atmospheric weapons testing took place as early as 1945, but mainly in the 1950s and early 1960s (Enting 1982), and we therefore cannot rule out these potential impacts on our localized record.

Our annual plant data also noticeably deviate from estimated tropospheric $^{14}CO_2$ in the last decade. Elevated ^{14}C values could be due to cleaner air (i.e., less local fossil fuel contributions) due to the remoteness, as well as high elevation (>2000 m) in much of the region we sampled. Elevated ^{14}C values may also be the result of increased wildfires in the western U.S. (Zhuang et al. 2021) and localized biomass burning due to recent forest management efforts, which re-introduce bomb ^{14}C (Randerson et al. 2002; Schuur et al. 2003; Heckman et al. 2013) into the atmosphere during the summer growing season.

Accurate dating of recent terrestrial organic matter require that we take these regional to local scale deviations in the annual plant data into consideration. This is particularly crucial for dating faster cycling organic matter pools, like plant respired carbon and stored mobile plant carbon pools, where deviations of just 2–4‰ in the local background atmosphere can impact the attribution of current year carbon versus previous year's carbon (Carbone et al. 2013).

Potential of Annual Plants as Widespread Samplers of Tropospheric $^{14}CO_2$

Annual plants have several characteristics that make them appealing to use as samplers of CO_2. These include: no carryover of nonstructural carbon pools from previous years, atmospheric integration times of weeks to months, and widespread abundance in both space (many are weeds or crops) and in time (due to herbaria collections and short lifespans). Our data additionally show that the genus of plant was not associated with any detectable bias in the measured ^{14}C, thus many species of annual plants may be available for this purpose. For terrestrial carbon cycling studies, annual plants record the $^{14}CO_2$ that the ecosystem (plants and soil) experience, and thus may be more accurate for dating or attributing sources than "free" atmospheric records.

There are also disadvantages to annual plants as samplers of $^{14}CO_2$ that lead to uncertainties that should be addressed. These include specimen curation and preparation that may introduce contamination to the ^{14}C measurement. However, the primary disadvantage we encountered in this analysis was uncertain sampling integration time. Most annual plants have short lifespans of 1–3 months, but up to 6 months; herbarium records indicate the date of collection but provide no information about when the plant germinated. An individual leaf could integrate carbon from the atmosphere over just weeks. Determining this integration time for individual plant types and tissues would be important for higher time resolution records. This integration time may depend on how much plant tissue can be sampled for ^{14}C, i.e., whether the whole plant is being sampled or just a few leaves. Alternatively, for certain applications, annual plants could be purposely grown from seeds (e.g., "iso-meters;" Körner et al. 2005; Carbone et al. 2016), and the observed period of growth used to estimate the atmospheric integration time more accurately. More detailed understanding of how the ^{14}C of the atmospheric is incorporated into different annual plant tissues of stems, leaves, flowers, seeds, and their nonstructural carbon, could better inform the use of herbaria data for new records. We also note that tree ring records may have much larger integration time uncertainty than annual plants, as tree nonstructural carbohydrate pools stored in bole tissue integrate years of photosynthetic activity (Carbone et al. 2013; Richardson et al. 2013).

We believe the ease of sampling and positive characteristics discussed above largely outweigh this time integration uncertainty and provide exciting potential for the use of annuals plants as widespread samplers of the past and future $^{14}CO_2$. Utilizing large numbers of herbarium collections that extend decades to centuries into the past (Lang et al. 2019) could allow for expansion to higher time resolution and greater spatial representation of $^{14}CO_2$ records, and mapping of local-to-regional deviations from the hemispherical averages. Since AMS samples sizes can be very small, the amount of tissue collected should not present a problem for most herbarium specimens. Also, many herbaria recognize the value of allowing specimens to be subsampled for chemical and genomic analyses, as long as specimens are properly annotated. Finally, because many herbarium collections can be queried remotely online the time and effort required to identify potential specimens is, remarkably, quite minimal. Future sampling campaigns of annual plants could also include annual plants as recorders of the fossil fuel imprint on specific locations for carbon accounting purposes. Finally, we note that in addition to calls for increased high resolution flask sampling (Levin et al. 2022) annual plants could potentially complement information used to constrain Earth System Models (Graven et al. 2017) to understand global and regional scale exchange fluxes of the modern carbon cycle.

CONCLUSIONS

We used 100 annual plants that grew between 1910 and 2021 as a “proof of concept” to create a record of $^{14}CO_2$ for the region near Flagstaff, Arizona, USA. This record is dominated by five commonly occurring annual plant species in the area, and most samples were previously archived herbarium specimens. We provide a localized synthetic record from which dating of recent terrestrial organic matter tissues and pools may be more accurate than synthetic global records. With increasing access to, and decreasing costs in AMS analyses, our results highlight the potential of planted and wild annual vegetation, as well as archived in herbarium collections, for increased time and spatial resolution of ^{14}C records.

ACKNOWLEDGMENTS

We thank A.Z. Richardson for expert assistance with 2017–2021 annual plant identification and harvesting. NSF grant #1919506 provided AGE3 instrumentation to graphitize annual plants for AMS analyses. We gratefully acknowledge the financial support of the Office of the President and Vice President of Research at Northern Arizona University for support in acquiring the MICADAS. Any use of trade, product, or firm names in this paper is for descriptive purposes only and does not imply endorsement by the U.S. Government. We thank Q. Hua and two anonymous reviewers for their helpful feedback in revising this manuscript.

SUPPLEMENTARY MATERIAL

To view supplementary material for this article, please visit https://doi.org/10.1017/RDC.2023.5

REFERENCES

Berger R, Fergusson GJ, Libby WF. 1965. UCLA radiocarbon dates IV. Radiocarbon 7:336–371.

Berger R, Jackson TB, Michael R, Suess HE. 1987. Radiocarbon content of tropospheric CO_2 at China Lake, California 1977–1983. Radiocarbon 29(1):18–23.

Berger R, Libby WF. 1966. UCLA radiocarbon dates V. Radiocarbon 8:467–497.

Berger R, Libby WF. 1967. UCLA radiocarbon dates VI. Radiocarbon 9:477–504.

Berger R, Libby WF. 1968. UCLA radiocarbon dates VIII. Radiocarbon 10(2):402–416.

Berger R, Libby WF. 1969. UCLA radiocarbon dates IX. Radiocarbon 11(1):194–209.

Broecker WS, Peng T-H, Ostlund G, Stuiver M. 1985. The distribution of bomb radiocarbon in the ocean. Journal of Geophysical Research 90(C4):6953–6970. doi: 10.1029/jc090ic04p06953.

Cain WF, Griffin S, Druffel-Rodriguez KC, Druffel ERM. 2018. Uptake of carbon for cellulose production in a white oak from western Oregon, USA. Radiocarbon 60(1):151–158. doi: 10.1017/RDC.2017.82.

Carbone MS, Czimczik CI, Keenan TF, et al. 2013. Age, allocation and availability of nonstructural carbon in mature red maple trees. New Phytol. 200(4). doi: 10.1111/nph.12448.

Carbone MS, Richardson AD, Chen M, Davidson EA, Hughes H, Savage KE, Hollinger DY. 2016. Constrained partitioning of autotrophic and heterotrophic respiration reduces model uncertainties of forest ecosystem carbon fluxes but not stocks. Journal of Geophysical Research: Biogeosciences 121(9). doi: 10.1002/2016JG003386.

Druffel EM, Suess HE. 1983. On the radiocarbon record in banded corals: exchange parameters and net transport of $^{14}CO_2$ between atmosphere and surface ocean. Journal of Geophysical Research 88(C2). doi: 10.1029/JC088iC02p01271.

Enting IG. 1982. Nuclear weapons data for use in carbon cycle modeling. CSIRO Division of Atmospheric Physics Technical Paper No. 44. Melbourne: CSIRO.

Furze ME, Huggett BA, Aubrecht DM, Stolz CD, Carbone MS, Richardson AD. 2018. Whole-tree nonstructural carbohydrate storage and seasonal dynamics in five temperate species. New Phytologist.

Furze ME, Huggett BA, Chamberlain CJ, et al. 2020. Seasonal fluctuation of nonstructural carbohydrates reveals the metabolic availability of stemwood reserves in temperate trees with contrasting wood anatomy. Tree Physiology 40(10). doi: 10.1093/treephys/tpaa080.

Godwin H. 1969. The value of plant materials for radiocarbon dating. American Journal of Botany 56(7):723. doi: 10.2307/2440592.

Graven H, Allison CE, Etheridge DM, et al. 2017. Compiled records of carbon isotopes in atmospheric CO_2 for historical simulations in CMIP6. Geoscientific Model Development 10(12). doi: 10.5194/gmd-104405-2017.

Grootes PM, Farwell GW, Schmidt FH, Leach DD, Stuiver M. 1989. Rapid response of tree cellulose radiocarbon content to changes in atmospheric $^{14}CO_2$ concentration. Tellus 41B:134–148.

Heckman K, Campbell J, Powers H, Law B, Swanston C. 2013. The influence of fire on the radiocarbon signature and character of soil organic matter in the Siskiyou national forest, Oregon, USA. Fire Ecology 9(2). doi: 10.4996/fireecology.0902040.

Hesshaimer V, Heimann M, Levin I. 1994. Radiocarbon evidence for a smaller oceanic carbon dioxide sink than previously believed. Nature 370(6486):201–203. doi: 10.1038/370201a0.

Hesshaimer V, Levin I. 2000. Revision of the stratospheric bomb $^{14}CO_2$ inventory. Journal of Geophysical Research Atmos. 105(D9). doi: 10.1029/1999JD901134.

Hsueh DY, Krakauer NY, Randerson JT, Xu X, Trumbore SE, Southon JR. 2007. Regional patterns of radiocarbon and fossil fuel-derived CO_2 in surface air across North America. Geophysical Research Letters 34(2). doi: 10.1029/2006GL027032.

Hua Q, Barbetti, M. 2004. Review of tropospheric bomb ^{14}C data for carbon cycle modeling and age calibration purposes. Radiocarbon 46(3): 1273–1298. doi: 10.1017/S0033822200033142.

Hua Q, Barbetti M, Rakowski AZ. 2013. Atmospheric radiocarbon for the period 1950–2010. Radiocarbon 55(4). doi: 10.2458/azu_js_rc.v55i2.16177.

Hua Q, Turnbull JC, Santos GM, et al. 2022. Atmospheric radiocarbon for the period 1950–2019. Radiocarbon. doi:10.1017/RDC.2021.95.

Hüls C, Börner AM, Hamann C. 2021. Wheat seed (*Triticum aestivum* L.) Radiocarbon concentration over the last 75 years. Radiocarbon 63(5). doi: 10.1017/RDC.2021.81.

Keeling CD. 1979. The Suess effect: 13Carbon-14Carbon interrelations. Environment International 2(4–6):229–300. doi: 10.1016/0160-4120(79)90005-9.

Körner C, Asshoff R, Bignucolo O, et al. 2005. Carbon flux and growth in mature deciduous forest trees exposed to elevated CO2. Science (80):309(5739):1360–1362.

Lang PLM, Willems FM, Scheepens JF, Burbano HA, Bossdorf O. 2019. Using herbaria to study global environmental change. New Phytologist 221(1). doi: 10.1111/nph.15401.

Levin I, Hammer S, Kromer B, Preunkert S, Weller R, Worthy DE. 2022. Radiocarbon in global tropospheric carbon dioxide. Radiocarbon. doi:10.1017/RDC.2021.102.

Levin I, Kromer B. 1997. Twenty years of atmospheric $^{14}CO_2$ observations at Schauinsland Station, Germany. Radiocarbon 39(2):205–218. doi: 10.1017/S0033822200052012.

Liu Z, Ciais P, Deng Z, et al. 2020. Near-real-time monitoring of global CO_2 emissions reveals the effects of the COVID-19 pandemic. Nature Communications 11(1). doi: 10.1038/s41467-020-18922-7.

McDonald L, Chivall D, Miles D, Bronk Ramsey C. 2019. Seasonal variations in the ^{14}C Content of tree rings: influences on radiocarbon calibration and single-year curve construction. Radiocarbon 61(1):185–194. doi: 10.1017/RDC.2018.64.

Meineke EK, Classen AT, Sanders NJ, Jonathan Davies T. 2019. Herbarium specimens reveal increasing herbivory over the past century. Journal of Ecology 107(1). doi: 10.1111/1365-2745.13057.

Meineke EK, Davis CC, Davies TJ. 2018. The unrealized potential of herbaria for global change biology. Ecological Monographs 88(4). doi: 10.1002/ecm.1307.

Peñuelas J, Azcón-Bieto J. 1992. Changes in leaf $\Delta^{13}C$ of herbarium plant species during the last 3 centuries of CO_2 increase. Plant, Cell & Environment 15(4). doi: 10.1111/j.1365-3040.1992.tb01000.x.

Randerson JT, Enting IG, Schuur EAG, Caldeira K, Fung IY. 2002. Seasonal and latitudinal variability of troposphere $\Delta^{14}CO_2$: post bomb contributions from fossil fuels, oceans, the stratosphere, and the terrestrial biosphere. Global Biogeochemical Cycles 16(4):1112. doi: 10.1029/2002GB001876.

Reid J. 2014. The "great migration" in Northern Arizona: 1940–1960. Journal of Arizona History: 469–498.

Revelle R, Suess HE. 1957. Carbon dioxide exchange between atmosphere and ocean and the question of an increase of atmospheric CO_2 during the past decades. Tellus 9(1). doi: 10.3402/tellusa.v9i1.9075.

Richardson AD, Carbone MS, Keenan TF, et al. 2013. Seasonal dynamics and age of stemwood nonstructural carbohydrates in temperate forest trees. New Phytolgist 197(3). doi: 10.1111/nph.12042

Riley WJ, Hsueh DY, Randerson JT, et al. 2008. Where do fossil fuel carbon dioxide emissions from California go? An analysis based on radiocarbon observations and an atmospheric transport model. Journal of Geophysical Research Biogeosciences 113(4). doi: 10.1029/2007JG000625.

Schuur EAG, Trumbore SE, Mack MC, Harden JW. 2003. Isotopic composition of carbon dioxide from a boreal forest fire: Inferring carbon loss from measurements and modeling. Global Biogeochemical Cycles 17(1). doi: 10.1029/2001gb001840.

Stuiver M, Quay PD. 1981. Atmospheric ^{14}C changes resulting from fossil fuel CO_2 release and cosmic ray flux variability. Earth Planet Science Letters 53(3):349–362. doi: 10.1016/0012-821X(81)90040-6.

Suess HE. 1955. Radiocarbon concentration in modern wood. Science (80):122(3166). doi:10.1126/science.122.3166.415-a.

Telegadas K. 1971. The seasonal atmospheric distribution and inventories of excess carbon-14 from March 1955 to July 1969, HASL-243. New York: Health and Safety Lab., U.S. Atomic Energy Commission. p. 2–86.

Thiers BM. 2022. Index herbariorum. Available at: http://sweetgum.nybg.org/science/ih/. Last accessed 2 Dec. 2022.

Trumbore S. 2000. Age of soil organic matter and soil respiration: radiocarbon constraints on belowground C dynamics. Ecological Applications 10(2):399–411.

Trumbore SE, Sierra CA, Hicks Pries CE. 2016. Radiocarbon nomenclature, theory, models, and interpretation: measuring age, determining cycling rates, and tracing source pools. In: Radiocarbon and climate change. Springer Cham, Springer International Publishing. p. 45–82. doi:10.1007/978-3-319-25643-6_3.

Turnbull JC, Mikaloff Fletcher SE, Ansell I, et al. 2017. Sixty years of radiocarbon dioxide measurements at Wellington, New Zealand: 1954–2014. Atmospheric Chemistry and Physics 17(23):14771–14784. doi: 10.5194/acp-17-14771-2017.

Turney CSM, Palmer J, Maslin MA, Hogg A, Fogwill CJ, Southon J, Fenwick P, Helle G, Wilmshurst JM, McGlone M, Bronk Ramsey C, Thomas Z, Lipson M, Beaven B, Jones RT, Andrews O, Hua Q. 2018. Global peak in atmospheric radiocarbon provides a potential definition for the onset of the Anthropocene epoch in 1965. Scientific Reports 8(1).

Wang W, Pataki DE. 2010. Spatial patterns of plant isotope tracers in the Los Angeles urban region. Landscape Ecology 25(1):35–52. doi: 10.1007/s10980-009-9401-5.

Wang W, Pataki DE. 2012. Drivers of spatial variability in urban plant and soil isotopic composition in the Los Angeles basin. Plant and Soil 350(1–2):323–338. doi: 10.1007/s11104-011-0912-x.

Willis CG, Ellwood ER, Primack RB, et al. 2017. Old plants, new tricks: phenological research using herbarium specimens. Trends in Ecology & Evolution 32(7). doi: 10.1016/j.tree.2017.03.015.

Woodward FI. 1987. Stomatal numbers are sensitive to increases in CO_2 from pre-industrial levels. Nature 327(6123). doi: 10.1038/327617a0.

Yamada Y, Yasuike K, Komura K. 2005. Temporal variation of Carbon-14 concentration in tree-ring cellulose for the recent 50 years. Journal of Nuclear and Radiochemical Sciences 6(2):135–138. doi: 10.14494/jnrs2000.6.2_135.

Zhuang Y, Fu R, Santer BD, Dickinson RE, Hall A. 2021. Quantifying contributions of natural variability and anthropogenic forcings on increased fire weather risk over the western United States. PNAS 18(45). doi: 10.1073/pnas.2111875118.